Electrostatic fields and compositional fluctuations in (In,Ga)N/GaN multiple quantum wells grown by plasma-assisted molecular-beam epitaxy

Patrick Waltereit,* Oliver Brandt, Jens Ringling,† and Klaus H. Ploog
Paul-Drude-Institut für Festkörperelektronik, Hausvogteiplatz 5–7, D-10117 Berlin, Germany
(Received 11 April 2001; revised manuscript received 6 August 2001; published 28 November 2001)

We investigate the recombination mechanism in (In,Ga)N/GaN multiple quantum wells grown by plasma-assisted molecular-beam epitaxy. It is shown that for a thorough understanding of the spontaneous emission from these structures both electrostatic fields and compositional fluctuations have to be taken into account. The influence of the internal electrostatic fields is examined by continuous-wave and time-resolved photoluminescence as a function of well width. The transition energies and radiative decay times are shown to be in agreement with the quantum-confined Stark effect in these structures. The temperature dependence of the radiative decay time is measured to probe the dimensionality of the system. For a quantitative understanding, a rate-equation model is utilized for analyzing the data. At low temperatures, recombination is governed by localized states whereas for high temperatures extended states dominate. This analysis shows that the localization depth in these structures is below 25 meV.

DOI: 10.1103/PhysRevB.64.245305 PACS number(s): 81.05.Ea, 81.15.Hi, 64.75.+g

I. INTRODUCTION

Despite the successful demonstration of (In,Ga)N/GaN multiple quantum well (MQW) light emitting diodes and injection laser diodes, there still is a lack of agreement about the actual recombination mechanisms in these structures. The experimental results[1–5] are controversially discussed in terms of two different phenomena, namely, internal electrostatic fields and compositional fluctuations. This controversy may be due to the fact that the consequences of compositional fluctuations are difficult to distinguish from those of internal electrostatic fields, as detailed in the following.

The strong polarization fields in wurtzite nitride semiconductors[6] lead to the formation of huge electrostatic fields parallel to the polar *c* axis of [0001] oriented (Al,Ga,In)N heterostructures.[7] These fields result in the spatial separation of electrons and holes and thus in a redshift of transition energies (quantum-confined Stark effect) and prolonged radiative decay times with respect to flat band conditions.[8]

In thermal equilibrium, a miscibility gap is predicted on theoretical grounds for (In,Ga)N leading to spinodal decomposition (bulk segregation).[9] While the deposition temperatures for both molecular-beam epitaxy (MBE) and metal-organic chemical-vapor deposition are far too low for achieving thermal equilibrium, compositional inhomogeneities and In clustering has been observed for this material.[10,11] Excitons will be localized at regions having a higher In content with respect to the surrounding matrix. The larger the localization depth, the more the transition energy is redshifted and the transition rate is reduced with respect to the free exciton.[12] In the experiment, these findings coincide with the consequences of internal electrostatic fields.

Therefore it is impossible to distinguish electrostatic fields and compositional fluctuations by a single photoluminescence (PL) experiment. Absorption measurements also fail to distinguish between these two phenomena since the oscillator strength is substantially reduced in both cases. Transitions with higher energy have a larger oscillator strength and thus a Stokes-like shift between emission and absorption is commonly observed.[13] Indeed, this shift is rightly called apparent Stokes shift, acknowledging the fact that the ground state with its extremely low oscillator strength is simply undetectable in absorption.

In this paper, we will devise and demonstrate experiments which allow us to distinguish between these two phenomena. A separation of fields and fluctuations is possible by variations of parameters to which only either of these phenomena is sensitive. Specifically, we will tune an internal parameter (well width) and an external parameter (PL measurement temperature) to access electrostatic fields and compositional fluctuations, respectively.

(In,Ga)N wells grown under nominally identical conditions are expected to exhibit very similar degrees of compositional inhomogeneity. Hence the impact of electrostatic fields may be investigated by varying only the individual thicknesses of well and barrier but keeping the In content in the well constant. The resulting changes in emission energy and decay time may then be assigned to electrostatic fields with confidence. However, the examination of samples having different well widths relies on the reproducibility of the growth procedure. In segregation, desorption and clustering are all thermally activated processes and thus critically depend on the deposition temperature. Instabilities of the latter may lead to substantial deviations of the transition energies of samples grown under nominally identical conditions. For example, the transition energy is reported to shift as much as 250 meV by variations of only 10 K of the substrate temperature.[14] For examining the reproducibility of our own growth procedure, we investigated two samples grown at different days under nominally exactly identical conditions. We found both the structural and optical properties of these two samples to be in close agreement. The In content, as determined by x-ray diffractometry, differed by only 1%, and the PL peak position at 5 K was shifted by less than 50 meV. These figures thus set the error margin for comparison of different samples.

Direct access to compositional fluctuations is possible by investigation of the dimensionality of the system at different temperatures. At very low temperatures, excitons are localized and occupy zero-dimensional states. With increasing

temperature, excitons are thermally activated and start to occupy extended, two-dimensional states of the quantum well. A quantity reflecting the dimensionality of the system is the radiative decay time τ_r which is proportional to $T^{s/2}$ for a system having s dimensions.[15]

II. EXPERIMENT

The samples are grown on on-axis Si-face SiC(0001) by plasma-assisted MBE in a modified Riber-32 system equipped with conventional effusion cells for Ga and In and an EPI RF N-plasma source. Approximately 1-μm-thick GaN(0001) buffer layers are grown prior to the deposition of the actual MQW structure at a substrate temperature of about 700 °C and stoichiometric conditions. Further details of substrate preparation and buffer growth may be found elsewhere.[16] The deposition of the (In,Ga)N/GaN MQW structure requires a lower substrate temperature as well as a higher flux of active N with respect to the GaN buffer. Hence, prior to the growth of the (In,Ga)N/GaN MQW structure, growth is interrupted for approximately 15 min for decreasing the substrate temperature and for stabilizing a high N flux. The (In,Ga)N/GaN MQW's are then deposited at a substrate temperature of 580 °C, a plasma power of up to 250 W, and a N_2 flow of 0.7 SCCM (SCCM denotes cubic centimeter per minute at STP), yielding a N-limited growth rate well in excess of 1 μm/h. Growth is monitored *in situ* by reflection high-energy electron diffraction (RHEED). After growth, the samples are characterized by high-resolution triple-axis $\theta-2\theta$ x-ray diffraction (HRXRD) scans using $Cu_{K\alpha_1}$ radiation. The profiles thus obtained are analyzed by dynamical x-ray-diffraction simulations valid for arbitrarily high strain.[17] The optical properties are studied by continuous-wave PL (cw PL) using the 325-nm line of a He-Cd laser at an excitation density of 0.1 W cm^{-2} and time-resolved PL (TRPL) utilizing a frequency-tripled Ti:sapphire laser with a pulse width of about 400 fs, a repetition rate of 76 MHz, and a fluence of 1 nJ cm^{-2}.

III. SAMPLE STRUCTURE

The samples investigated in this work are labeled W1 and W2 and consist of ten-period (In,Ga)N/GaN MQW's. In these samples, the layer thicknesses are varied utilizing different well deposition times but otherwise nominally identical growth conditions. Metal-stable surface stoichiometries were used to achieve smooth interfaces in order to minimize the localization of carriers at well width fluctuations induced by N-stable conditions. Such a localization leads to a significant redshift of the transition energy.[18]

The structural parameters of the two MQW's are examined in analogy to our recent work[18] which is summarized in the following. During QW growth, a (1×1) RHEED pattern is observed, which gains in intensity during barrier growth until finally a transition to a threefold reconstruction along the [1100] azimuth is detected. The time delay for the appearance of the surface reconstruction depends on the specific surface stoichiometries during well and barrier deposition. Large V/III ratios lead to short time delays and vice versa. As large V/III ratios are known to suppress In segregation in (In,Ga)N growth, it is tempting to explain the time delay by the presence of a floating In layer that is consumed during barrier deposition. The presence of In segregation for metal-rich grown wells is seen in HRXRD in conjunction with dynamical simulation. In HRXRD, only the integrated In content is determined and the kinematic analysis based on the nominal deposition times yields the nominal MQW parameters. However, the simulation based on these nominal parameters fails to agree with the data. Interestingly, excellent agreement is obtained after kinematic analysis with the sum of nominal deposition time and delay time taken from RHEED to account for In segregation. Secondary-ion mass spectroscopy (SIMS) supports this approach as the actual well thickness is in very good agreement with the structural parameters determined using the modified deposition times. The interfaces of the samples under investigation in this paper are indeed smooth, as evidenced by a streaky RHEED pattern during growth and the agreement of the experimental and simulated satellite peak intensities and linewidths in HRXRD.

TABLE I. Structural parameters of the two (In,Ga)N/GaN MQW's as determined by x-ray diffraction. x, d_{InGaN}, and d_{GaN} denote the In content in the well, the well thickness, and the barrier thickness, respectively.

Sample	x	d_{InGaN} (nm)	d_{GaN} (nm)
W1	0.17	3.1	12.1
W2	0.16	5.9	8.8

As seen from the structural data (Table I), the two samples have nearly identical MQW periods (15 nm) and In contents (0.16) in the well. These samples are thus ideally suited for a direct investigation of electrostatic fields as only the well width varies. It should be noted in this context that a direct kinematical analysis of the XRD profiles (neglecting In segregation) yields twice the In content and only half the well width with respect to the values in Table I.

IV. ELECTROSTATIC FIELDS

Figure 1 compares the optical properties of samples W1 and W2 at 5 K. The transition energy of sample W1 with the 3.1-nm-wide wells is at 2.83 eV while that of sample W2 with its 5.9-nm-wide wells is redshifted to 2.48 eV. Moreover, the PL decay times are remarkably different. Sample W1 exhibits an almost monoexponential decay with a decay time of $\tau_{W1}=1$ ns. In contrast, sample W2 exhibits a significantly prolonged decay time τ_{W2}, which can only be roughly estimated to be $\tau_{W2}=50$ ns from the PL intensity ratio directly after and before the 13-ns separated excitation pulses under the assumption of a monoexponential decay.

For a direct comparison of these experimental results with theoretically expected transition energies the band profiles of these samples are calculated on the basis of the structural parameters in Table I. We perform self-consistent Schrödinger-Poisson calculations[19] using the piezoelectric and spontaneous polarization constants of Bernadini *et al.*[6] These band profiles (Fig. 2) are dominated by the presence of

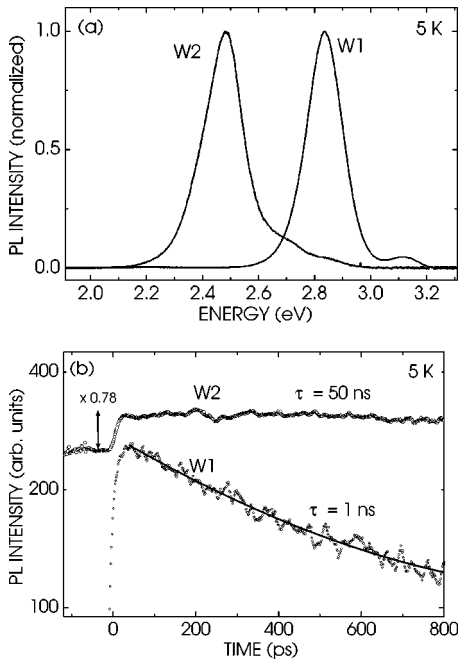

FIG. 1. Transition energy and decay time of the (In,Ga)N/GaN MQW's at 5 K studied by (a) cw PL and (b) TRPL. Note the redshift in transition energy and the prolonged decay time of sample W2 with respect to sample W1. The decay time of sample W2 is estimated from the PL intensity ratio of 0.78 prior and after the excitation pulse (sequential pulses are separated by 13 ns).

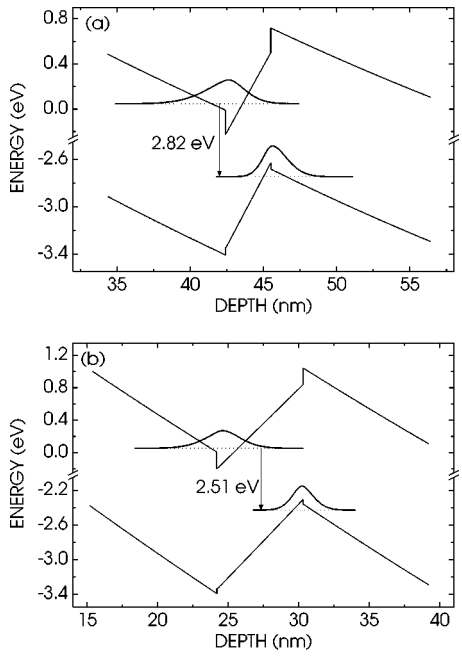

FIG. 2. Band profiles of the (In,Ga)N/GaN MQW under investigation for (a) sample W1 and (b) sample W2. The transition energies are given in the figure.

strong electrostatic fields in these structures. The estimated transition energies are in very good agreement with the data in Fig. 1 as the calculated transition energies are 2.82 and 2.51 eV for samples W1 and W2, respectively. Moreover, the ratio of the radiative decay times can be estimated from the respective electron and hole wave-function overlap. Theoretically, we expect $\tau_{W2}/\tau_{W1} \approx 110$ which is in fair agreement with the experimental value of 50 taking into account the experimental uncertainty in τ_{W2}. These findings clearly demonstrate that electrostatic fields play an important role for recombination and must not be neglected.

It is interesting to calculate the transition energies based on the structural parameters obtained by neglecting In segregation (see above). These values result in transition energies of 2.89 and 2.38 eV, which evidently are in disagreement with the experimental data. In this case, one thus might be tempted to conclude that the electrostatic fields calculated from the polarization fields of Bernadini *et al.*[6] are too large. Indeed, a reduction of the electrostatic fields by a factor of 2 leads to a better agreement, in that the difference in transition energies between the two samples is close to the experimentally observed value of 0.35 eV. This finding is in perfect accordance with our previous results.[18] Incorrect structural parameters for (In,Ga)N/GaN MQW's will lead to the (wrong) conclusion that the electrostatic fields are smaller than theoretically expected. Having the knowledge of the (at least approximately) structural parameters, we instead arrive at an excellent agreement between calculated and experimentally observed transition energies and decay times.

Regardless of these details, it is clear that strong internal electric fields are always present in (In,Ga)N/GaN MQW's. For investigating effects related to a possible compositional inhomogeneity, it is thus required to concentrate on structures for which the impact of these electric fields is minimized. We thus focus in the following on sample W1. The comparatively short decay time of 1 ns for this sample evidences that carrier recombination is not overly affected by the presence of electric fields, thanks to its 3-nm-thin wells.

V. COMPOSITIONAL FLUCTUATIONS

We first examine the dependence of the PL decay time τ_{PL} on emission energy [Fig. 3(a)]. The decay time is approximately 1 ns in the vicinity of the main peak but decreases to about 250 ps as the emission energy approaches a weak high-energy peak. Previous investigators have observed similar PL spectra as well as energy-dependent decay times, and have attributed the high-energy peak to extended quantum well states, while the dominant low-energy peak was thought to be due to deeply localized states.[20] However, we have performed detailed depth resolved cathodoluminescence (CL) which evidenced the high-energy emission to be localized at the MQW/buffer interface.[21] It is thus most likely that this high-energy peak originates from the first quantum well, which we believe to be highly doped due to the SIMS from GaN layers with several growth interruptions were at the detection limit (10^{17} cm^{-3}) during continous growth, but peaked at the positions where growth interruptions were made. Based on these results and the temporal duration of the growth interruption, the O concentration at the buffer/MQW interface, assumed to have a width of two monolayers, is estimated to be as high as 2.5×10^{19} cm^{-3}. Self-consistent Schrödinger-Poisson calculations show that this

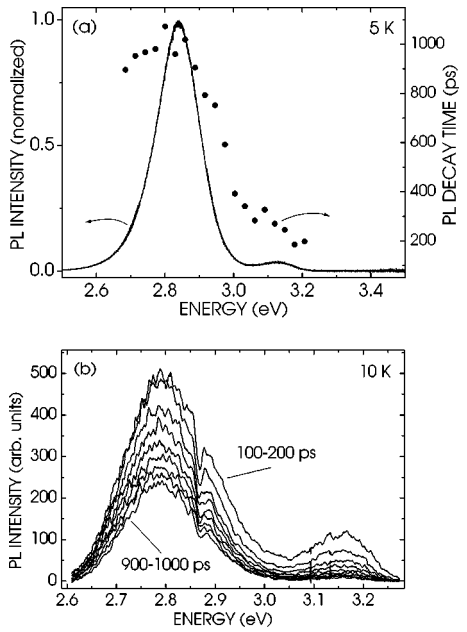

FIG. 3. TRPL decay of sample W1: (a) spectral dependence of the PL decay time, (b) transient spectra separated by 100 ps. The peak at 3.15 eV originates from the well closest to the GaN buffer as discussed in the text. The dip of the PL spectra at 2.85 eV is spurious.

concentration is sufficiently high to almost entirely screen the built-in electric field. The highly doped first well, which is in principle undesired, may thus even be viewed as an advantage: it may serve as a reference for field-free structures with regard to both transition energy and decay time. Furthermore, this interpretation explains why our single quantum well structures, grown under nominally identical conditions as their MQW counterparts, always emit at significantly higher energy: they simply correspond to the first, heavily doped first well of the MQW. In the following, we will focus on the dominant low-energy peak which represents the majority of the MQW structure.

The high-energy side of this main PL band shifts to the red in the course of time [Fig. 3(b)], causing an overall spectral narrowing of this band. Immediately after the excitation the linewidth is about 200 meV but then decreases to about 140 meV. These findings are consistent with a progressive relaxation of carriers into the states associated with the main emission band.

We now investigate the temperature dependence of the radiative decay time τ_r. Ideally, this value can be extracted from the combined measurement of the PL decay time $\tau(T)=(1/\tau_r+1/\tau_{nr})^{-1}$ and the steady-state PL intensity $I_{PL}(T)=\eta_{PL}(T)I_{PL}(0)$, with the quantum efficiency $\eta_{PL}(T)=\tau_{PL}/\tau_r$ and the nonradiative decay time τ_{nr}. Note that the dynamics of the transients may not be sufficient to accurately determine the PL decay time up to room temperature. Furthermore, we face bi- or multiexponential decays for higher temperatures which are characteristic of capture processes. Therefore the question arises which value to take for τ_{PL}.

We circumvent these ambiguities here by noting that the

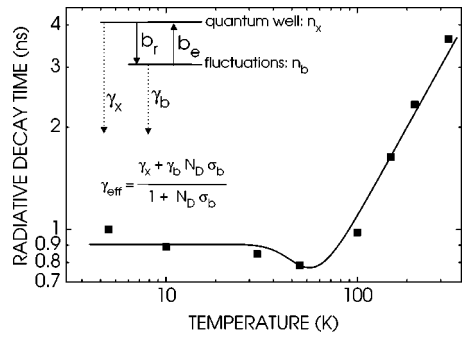

FIG. 4. Measured (symbols) and fit (line) radiative lifetimes vs temperature for the main peak of sample W1.

radiative decay time τ_r is proportional to the inverse of the spectrally integrated TRPL peak intensity divided by the incident fluence. This result can be derived as follows. Consider an excitation pulse $G(t)$ which generates excess carriers of density n_{GaN} in the GaN barriers. These carriers will relax to the (In,Ga)N wells with a relaxation time τ_{rel} establishing a density $n_{(In,Ga)N}$ in the well. The temporal evolution of these excess carrier densities is governed by the rate equations

$$\frac{d}{dt}n_{GaN}=G(t)-\frac{n_{GaN}}{\tau_{rel}}, \tag{5.1}$$

$$\frac{d}{dt}n_{(In,Ga)N}=+\frac{n_{GaN}}{\tau_{rel}}-\frac{n_{(In,Ga)N}}{\tau_r}-\frac{n_{(In,Ga)N}}{\tau_{nr}}. \tag{5.2}$$

For a Gaussian shaped excitation pulse $G(t)$ with a pulse width Δt, these coupled equations can be solved analytically under the boundary condition of zero excess carriers prior to the excitation pulse. If both Δt and τ_{rel} are small compared to any recombination process in the sample, it can be shown that the peak PL intensity of the transient is proportional to τ_r^{-1}. In the present case, both conditions are fulfilled. The pulse width is around 400 fs whereas the PL rise time sets an upper limit of 10 ps for the relaxation time τ_{rel}.

The radiative decay time is thus proportional to the rise of the spectrally PL transient intensity right after the exciting pulse [see the transient for sample W1 at 5 K in Fig. 1(b)]. The constant of proportionality is extracted by assigning an absolute value for τ_r at some temperature. We choose the value of τ_{PL}, at 5 K as here the decay is monoexponential apart from a very short initial capture process.

The corresponding values for $\tau_r(T)$ are shown in Fig. 4 together with a fit based on a rate-equation model to the data (the model follows the approach originally developed for thick GaN layers[22]). The radiative decay time is nearly independent of temperature below 80 K and then increases linearly with temperature. This observation evidences that recombination at low temperatures is governed by localized (zero-dimensional) states whereas emission at room temperature is dominated by extended (two-dimensional) states.

In order to further examine this result we develop a quantitative model for the recombination in the structures under investigation. The present model is based on the assumption

that radiative recombination is possible from either extended states in an ideal quantum well (2D states with occupation density n_x) or localized states (0D states with occupation density n_b). Transfer between these two kinds of states is incorporated by coupling terms. The temporal evolution of the corresponding occupation densities is described for the present case of excitonic recombination in the small-signal limit (note the very low excitation fluence of 1 nJ cm^{-2}) by the rate equations

$$dn_x/dt = -\gamma_x n_x - b_r n_x N_F + b_e n_b, \tag{5.3}$$

$$dn_b/dt = -\gamma_b n_b + b_r n_x N_F - b_e n_b, \tag{5.4}$$

where γ_x and γ_b are radiative recombination coefficients. The two other terms describe the capture (b_r) and emission (b_e) of localized excitons. N_F denotes the density of unoccupied localized states with a total density of $N_L = N_F + n_b$ of localized states available.

First, we consider the equilibrium occupation densities n_b^0 and n_x^0. The present situation constitutes a classical two-level systems with states $|F\rangle$ and $|b\rangle$. The former corresponds to an empty localized state with a density N_F^0 while the latter refers to an occupied localized state with a density n_b^0. Note that the occupied state has a lower energy than the empty state.

In equilibrium, we have

$$N_F^0 = n_b^0 e^{-E_{loc}/kT}, \quad n_x^0 = N_x e^{-E_x/kT} \tag{5.5}$$

with the localization energy E_{loc}, the total effective density of extended states N_x ($T \times 3.7 \times 10^{10}$ cm^{-2} K^{-1}), and the exciton binding energy E_x (26 meV).

Using the detailed balance expression $b_r n_x^0 N_F^0 = b_e n_b^0$, we obtain the cross section

$$\sigma_b = \frac{b_r}{b_e} = \frac{1}{N_x} e^{E_b/kT} \tag{5.6}$$

for capture of an exciton by a localized state with the localization binding energy $E_b = E_{loc} - E_x$. Note that this definition of E_b is analogous to the binding energy of an exciton localized at a dopant.

Second, we consider the dynamic behavior of the system. Here, we assume that capture and emission processes are very fast compared to radiative transitions even after excitation ($b_e, b_r \gg \gamma_x, \gamma_b$). Hence $b_r n_x N_F \approx b_e n_b$. One obtains an expression which relates the density n_b of occupied localized states with the density n_x of occupied extended states:

$$n_b = \frac{n_x \sigma_b N_L}{1 + \sigma_b n_x}. \tag{5.7}$$

Third, we add Eqs. (5.3) and (5.4) and use expression (5.7) to obtain

$$\frac{dn_x}{dt} = \frac{-\gamma_x n_x - \dfrac{\gamma_b \sigma_b N_L n_x}{1+\sigma_b n_x}}{1 + \dfrac{N_L \sigma_b}{(1+\sigma_b n_x)^2}} \approx -\left[\frac{\gamma_x + \gamma_b \sigma_b N_L}{1 + N_L \sigma_b}\right] n_x = -\gamma_{eff} n_x, \tag{5.8}$$

where the small-signal limit $n_x \sigma_b \ll 1$ has been used, as the maximum excess carrier density in our experiments is around 10^{15} cm^{-3}.

The effective transition rate $\gamma_{eff} = \tau_{eff}^{-1}$ describes the common radiative transition rate of the whole system. It is easily seen that this expression mediates between the limiting cases of $\gamma_{eff} \to \gamma_b$ for $T \to 0$ and $\gamma_{eff} \to \gamma_x$ for $T \to \infty$ as well as of $\gamma_{eff} \to \gamma_x$ for $N_L \to 0$ and $\gamma_{eff} \to \gamma_b$ for $N_L \to \infty$. Furthermore, for $E_b \to \infty$ and $E_b \to 0$, the value of γ_{eff} approaches γ_b and γ_x, respectively. The decay rate γ_x of a free exciton is given by a_x/T, and γ_b is independent of temperature. The satisfactory fit to the data (Fig. 4) yields $E_b = (22 \pm 62)$ meV, $N_L = (3 \pm 43) \times 10^{10}$ cm^{-2}, $\gamma_b = (1.1 \pm 0.1)$ ns^{-1}, and $a_x = (88 \pm 20)$ ns^{-1} K. This localization depth is considerably smaller than the usually reported values (more than 100 meV).[23] It is clear from our model that such a deep localization would lead to a constant radiative decay time at least up to room temperature. The density of localized states N_L obtained corresponds to an average lateral separation of about 50 nm of the localized states. This length scale is in agreement with the absence of any lateral shift of the emission energy in CL since the lateral resolution in CL is well above this separation.

VI. CONCLUSION

Summarizing and concluding, the radiative recombination from (In,Ga)N/GaN MQW's was examined. It was demonstrated that both compositional fluctuations and electrostatic fields have to be taken into account for a thorough understanding of the emission from these structures. In the case of thin quantum wells with high In content, localization in potential fluctuations governs the recombination whereas electrostatic fields are dominant in the case of thick wells having a low In content. If quantum wells in between these limiting cases are considered, one has to take into account the coexistence of both effects to consistently interpret the results. The influence of the internal electrostatic fields was examined as a function of the well width. The transition energies and radiative decay times have been shown to be in agreement with the quantum-confined Stark effect in these structures. The temperature dependence of the radiative decay time was measured to probe the dimensionality of the system. For a quantitative understanding, a rate-equation model was utilized for analyzing the data. For low temperatures, recombination is governed by localized states whereas for high temperatures, extended states dominate. This analysis shows that the localization depth in these structures is below 25 meV.

ACKNOWLEDGMENTS

We thank Martin Reiche for the HRXRD scans and gratefully acknowledge financial support by the Volkswagen-Stiftung.

*Present address: Materials Department, University of California, Santa Barbara, CA 93106; Electronic address: patrick@engineering.ucsb.edu

†Present address: Lambda-Physik, Hans-Böckler-Straße 12, D-37079, Göttingen, Germany.

[1] T. Wang, D. Nakagawa, M. Lachab, T. Sugahara, and S. Sakai, Appl. Phys. Lett. **74**, 3128 (1999).

[2] P.G. Eliseev, P. Perlin, J. Lee, and M. Osiński, Appl. Phys. Lett. **71**, 569 (1997).

[3] Y.-H. Cho, G.H. Gainer, A.J. Fischer, J.J. Song, S. Keller, U.K. Mishra, and S.P. DenBaars, Appl. Phys. Lett. **73**, 1370 (1998).

[4] P. Perlin, C. Kisielowski, V. Iota, B.A. Weinstein, L. Mattos, N.A. Shapiro, J. Krueger, E.R. Weber, and J. Yang, Appl. Phys. Lett. **73**, 2778 (1998).

[5] K.L. Teo, J.S. Colton, P.Y. Yu, E.R. Weber, M.F. Li, W. Liu, K. Uchida, K. Tokunaga, N. Akutsu, and K. Matsumoto, Appl. Phys. Lett. **73**, 1697 (1998).

[6] F. Bernardini, V. Fiorentini, and D. Vanderbilt, Phys. Rev. B **56**, R10 024 (1997).

[7] R. Langer, J. Simon, V. Oritz, N.T. Pelekanos, A. Barski, R. Andre, and M. Godlewski, Appl. Phys. Lett. **74**, 3827 (1999).

[8] P. Waltereit, O. Brandt, A. Trampert, H.T. Grahn, J. Menniger, M. Ramsteiner, M. Reiche, and K.H. Ploog, Nature (London) **406**, 865 (2000).

[9] I. Ho and G.B. Stringfellow, Appl. Phys. Lett. **69**, 2701 (1996).

[10] D. Doppalapudi, S.N. Basu, K.F. Ludwig, and T.D. Moustakas, Appl. Phys. Lett. **84**, 1389 (1998).

[11] M.K. Behbehani, E.L. Piner, S.X. Liu, N.A. El-Masry, and S.M. Bedair, Appl. Phys. Lett. **75**, 2202 (1999).

[12] E.I. Rashba, Sov. Phys. Semicond. **8**, 807 (1975).

[13] B. Damilano, N. Grandjean, J. Massies, L. Siozade, and J. Leymarie, Appl. Phys. Lett. **77**, 1268 (2000).

[14] J.M. van Hove, P.P. Chow, A.M. Wowchak, J.J. Klaassen, R. Hickman, and C. Polley, J. Vac. Sci. Technol. B **16**, 1286 (1998).

[15] H. T. Grahn, *Introduction to Semiconductor Physics* (World Scientific, Singapore, 1999).

[16] O. Brandt, R. Muralidharan, P. Waltereit, A. Thamm, A. Trampert, H. von Kiedrowski, and K.H. Ploog, Appl. Phys. Lett. **75**, 4019 (1999).

[17] O. Brandt, P. Waltereit, and K. H. Ploog (unpublished).

[18] P. Waltereit, O. Brandt, K. H. Ploog, M. A. Tagliente, and L. Tapfer (unpublished).

[19] We use the freeware program 1D Poisson/Schrödinger by G. Snider; see http://www.nd.edu/~gsnider.

[20] Y. Narukawa, Y. Kawakami, S. Fujita, S. Fujita, and S. Nakamura, Phys. Rev. B **55**, R1938 (1997).

[21] U. Jahn, P. Waltereit, O. Brandt, and K. H. Ploog (unpublished).

[22] O. Brandt, J. Ringling, K.H. Ploog, H.-J. Wünsche, and F. Henneberger, Phys. Rev. B **58**, R15 977 (1998).

[23] S. Chichibu, T. Sota, K. Wada, and S. Nakamura, J. Vac. Sci. Technol. B **16**, 2204 (1998).